PROCEEDINGS, Thirty-Eighth Workshop on Geothermal Reservoir Engineering
Stanford University, Stanford, California, February 11-13, 2013
SGP-TR-198

RECENT DEVELOPMENTS AT THE RAFT RIVER GEOTHERMAL FIELD

Jacob Bradford[1], John McLennan[2], Joseph Moore[1], Douglas Glasby[3], Douglas Waters[4], Richard Kruwell[4], Alan Bailey[5], William Rickard[5], Kevin Bloomfield[6], and Dennis King[7]

[1]Energy & Geoscience Institute at the University of Utah, Salt Lake City, UT 84108, USA

[2]Department of Chemical Engineering, University of Utah, Salt Lake City, UT 84108, USA

[3]US Geothermal Inc., 1505 Tyrell Lane, Boise, ID 83706, USA

[4]Waters Petroleum LLC, 4824 Potter Crest Circle, Anchorage, AK 99516

[5]Geothermal Resource Group, St. Charles Place, Suite B, Palm Desert, CA 92211, USA

[6]APEX Petroleum Engineering, Inc., 2 Inverness Drive, Suite 201 Englewood CO 80112, USA

[7]Sandia National Laboratories, Albuquerque NM 87123, USA

e-mail: J.T.Bradford@utah.edu

ABSTRACT

The Raft River geothermal field, located in Cassia County in southwestern Idaho, is the site of a Department of Energy Enhanced Geothermal System project. U.S. Geothermal, Inc. currently produces about 11 MWe from Precambrian metamorphic rocks. These lie beneath ~5,000 ft of Quaternary and Tertiary volcaniclastic and volcanic deposits. Maximum temperatures range from 271^{o} F to 300^{o} F.

Well RRG-9 ST1, the well targeted for stimulation is located approximately 1 mile south of the main bore field. The open hole section of the well, from 5,551 to 5,900 ft MD, consists of Precambrian Elba Quartzite, the stimulation target, granite and minor diabase. Prior to setting the casing acoustic, gamma ray, and density logs were run. After completing the well, a step rate/step down test was conducted. The maximum injection rate achieved was 18 bpm at a wellhead pressure of 1,150 psig.

A borehole televiewer run in the open hole section showed evidence of more than eighty fractures. The majority of these fractures trend from N20^{o}W to N20^{o}E and dip from 40^{o} to 60^{o}W. Permeable fractures were encountered in the Elba Quartzite at 5,640-5,660 ft MD. Analysis of the injection test indicates that the minimum in-situ principal stress in this zone is 3,050-3,200 psi, corresponding to a fracture gradient of 0.59-0.62 psi/ft. A discrete fracture network model was developed using measured and inferred fracture orientations, distributions and dimensions.

A three-phase stimulation program is proposed for RRG-9 ST-1. During the first two stages, water at 140^{o}F, and later 40^{o}F, will be injected to pre-condition and thermally fracture the reservoir. The third stage will consist of a high rate, large volume conventional hydraulic stimulation.

INTRODUCTION

The Raft River geothermal field is located in the southern part of the Raft River Valley, 90 miles southwest of Pocatello in southern Idaho (Figure 1).

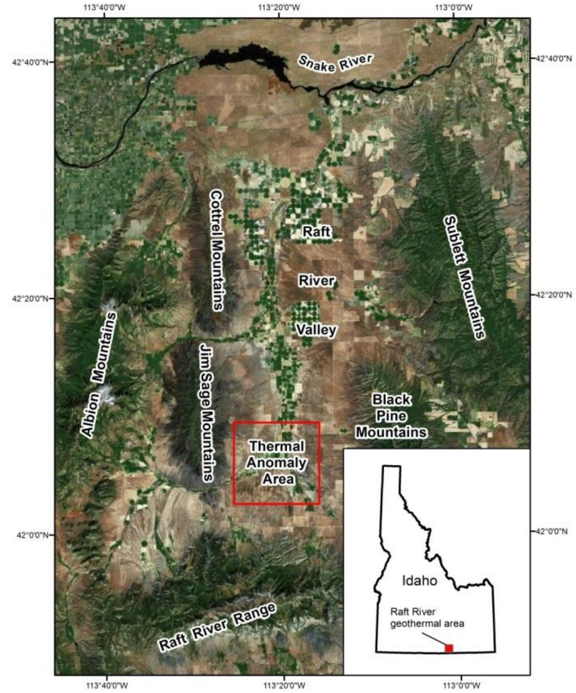

Figure 1: Raft River Geothermal Area.

The field is currently the site of a Department of Energy Enhanced Geothermal System project. It was initially developed between 1974 and 1982 by the Energy Research and Development Administration (ERDA) and later the US Department of Energy (DOE) as a geothermal demonstration project. Geophysical surveys were conducted and gradient, monitoring and seven full diameter production and injection wells were drilled. A 7 MW binary power plant was constructed and run for a short time. U.S. Geothermal acquired the property in 2002. Existing wells were deepened or sidetracked and several additional wells were drilled, including RRG-9; the well selected for upcoming stimulation (Figure 2).

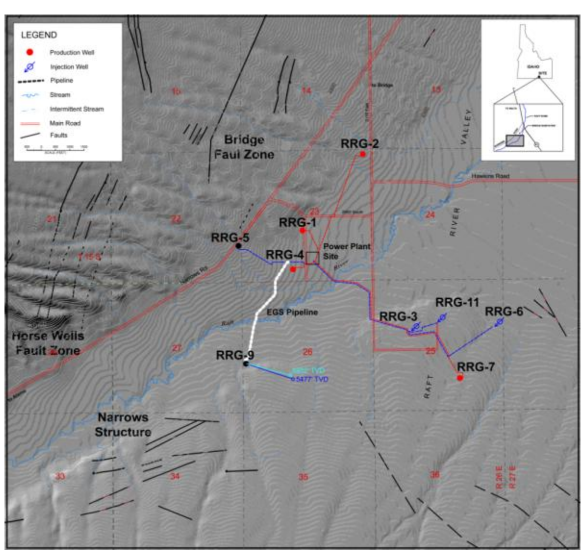

Figure 2: Location of Wells and Infrastructure at the Raft River Geothermal Site.

A 13 MW power plant was constructed and brought on line in 2007. U.S. Geothermal, Inc. currently produces between 10.5 and 11.5 megawatts from four production wells drilled into Precambrian metamorphic rocks. Bottomhole temperatures range from 271^{o} F to 300^{o} F. The produced fluids are NaCl waters with total dissolved solids ranging from 1,465 to 4,059 ppm. (Ayling and others, 2011)

GEOLOGIC SETTING

The Raft River Valley is located on the north-eastern edge of the Basin and Range province and on the southern side of the Snake River Plain. The geology is complex, reflecting the combined influences of these two geologic terrains. Deep wells drilled into the geothermal system within the Raft River Valley have encountered ~5,000 ft of discontinuous Quaternary and Tertiary volcaniclastic and volcanic rocks above the Precambrian metamorphic basement that hosts the geothermal reservoir. The primary reservoir is the Elba Quartzite. This is a fine-grained metamorphosed quartz-rich sandstone. A thin quartzite at the top of the metamorphic basement, schists, and quartz monzonite are also encountered in the deep wells. The Tertiary-Precambrian contact dips gently to the east and is inferred to be a detachment surface. Within the bore field, no major offset of this contact has been documented.

The Albion-Raft River-Grouse Creek metamorphic core complex and associated detachment faults - separating ductilly deformed footwall shear zones from brittle hanging wall rocks - dominates the regional structure. Covington (Covington, 1983) inferred that up to a 32,800 ft thickness of allochthonous Paleozoic and Mesozoic rock slices covered the entire area by the middle Oligocene. He further postulated that, by late Miocene, coherent gravity slide-blocks had moved about 15.5 miles eastwardly, away from the Albion Mountains, along the Raft River detachment fault.

Thrust faults, folds and easterly trending strike slip faults developed during the early Tertiary. These are exposed in the adjacent ranges (Covington, 1983). Normal faults cut Quaternary sediments (Figure. 3; Williams and others, 1974, 1976).

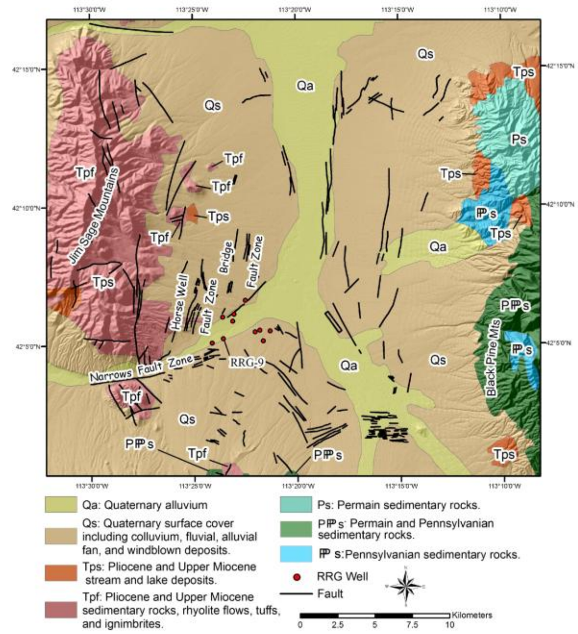

Figure 3: Surface geology map (after USGS, 2005; Link, 2002; Williams at al., 1974)

Two major fault zones have been identified on the west side of the Raft River valley. These are the Bridge Fault Zone and the Horse Wells Fault Zone. Both zones strike approximately north-south. These faults are inferred to be listric, normal faults, flattening at the basement-sediment contact. Production wells in the northwest part of the bore field are believed to intersect permeable zones associated with the Bridge Fault Zone. These faults terminate against the Narrows Zone, a poorly defined northeast-southwest trending structure represented by a linear resistivity low within the Precambrian rocks. The Narrows Zone appears to divide the geothermal system into two major compartments (Figure 4).

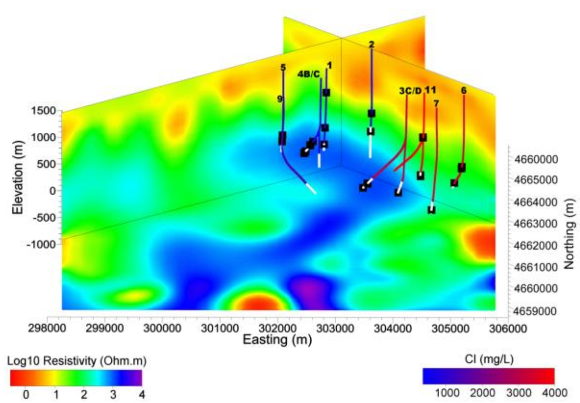

Figure 4: View of the Raft River field showing well deviations and the resistivity structure defined by magnetotelluric surveys. Black squares are lost circulation zones; white socks on show Precambrian rocks. The dark blue region in the center of the image is interpreted to represent the Narrows Zone. (Maris and others, 2012)

Wells drilled northwest of the Narrow Zone produce lower salinity waters from the Precambrian rocks than do wells to the southeast. The results of previous hydraulic fracturing and geologic mapping suggest that the Narrows Zone is also an important structural discontinuity within the Raft River geothermal field. Stimulation of well RRG-5, drilled northwest of the Narrows Zone produced a hydraulic fracture with a NNE trend (N29^{o}E; Keys, 1980) whereas stimulation of RRG-4, drilled southeast of the zone, produced a hydraulic fracture trending slightly north of east (N72^{o}E; Keys, 1980).

THE TARGET WELL: RRG-9 ST-1

For ongoing DOE-funded research, RRG-9 will be the target stimulation well. It was recently sidetracked and deepened to a measured depth (MD) of 5,932 ft. This inclined well is southwest of the main bore field and was originally drilled to test the intersection of the of the Narrows and Bridge Fault zones. The well was deviated to the east and cased to a depth of 2,317 ft MD. RRG-9 ST-1 was side-tracked and cased in 2012, in preparation of the stimulation experiments, after a failed attempt to deepen the original hole (Figure 5).

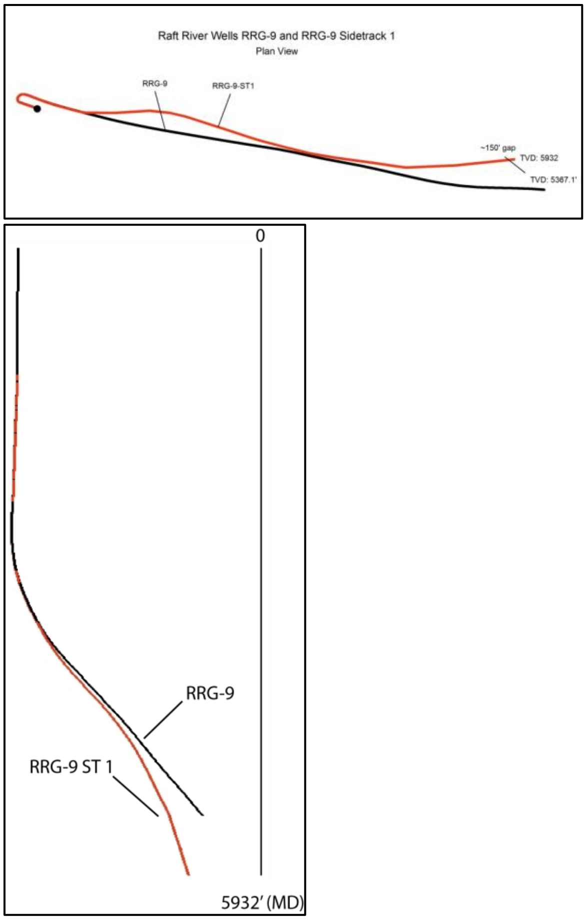

Figure 5: The relationship between RRG-9 and RRG-9 ST-1. Top: Plan view showing a view of the wells from above. Bottom: Side view showing the well deviations with depth. The two wells are located approximately 315 ft apart at TD.

RRG-9 ST-1 penetrated the Tertiary-Precambrian contact at 5,157 ft and the top of the Elba Quartzite at 5,299 ft (Figure 6).

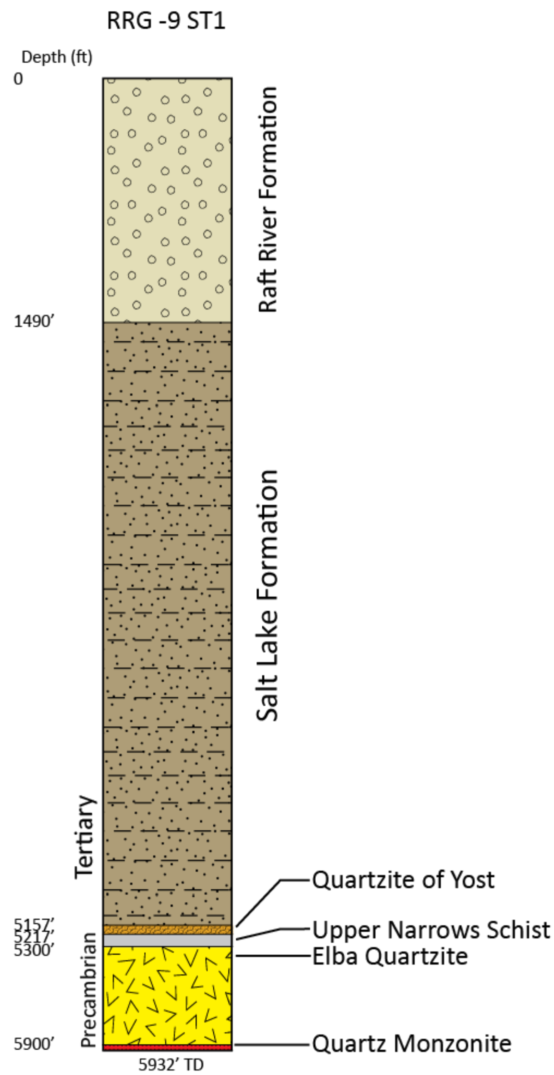

Figure 6: Formations around the RRG-9 ST-1 wellbore.

9 5/8" casing was set to a depth of 5,551 ft, approximately midway through the Elba Quartzite, after drilling the well to 5,561 ft. Prior to setting the casing, a deviation survey and acoustic, gamma, SP, and density logs were run. The well was completed in quartz monzonite.

RRG-9 ST-1 was completed at a depth of 5,932 ft in quartz monzonite. The base of the Elba Quartzite was encountered at 5,900 ft. No significant fluid losses were encountered during drilling. After drilling to TD, an injection test was conducted. Pressure, temperature and televiewer surveys were run prior to the injection test but only pressure and temperature were measured after the test. An unequilbrated temperature of 282°F was encountered at the base of the well.

PRELIMINARY STEP RATE/STEP DOWN STIMULATION RESULTS

After cementing, an injection program was carried out in the entire barefoot section of the hole. A step rate test was conducted to determine the stresses acting on the Elba Quartzite. 1,944 bbl of irrigation water were injected with rates up to 18 bbl per minute and a wellhead pressure of 1,150 psig. The injection test were carried out in two stages; a step rate test with increasingly higher pump rates followed by a step down test. The step down test started with higher injection rates and these were progressively reduced as the test progressed, (Figures, 7 and 8).

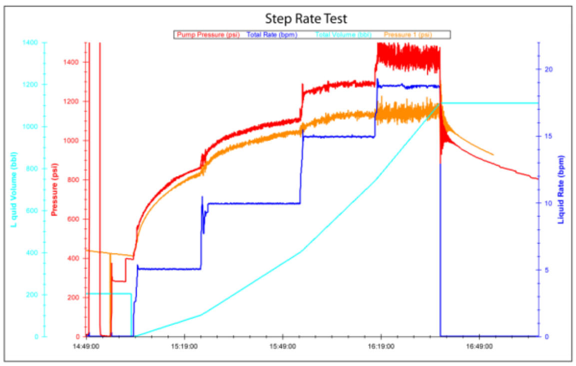

Figure 7: Step rate test conditions from 14:49 to 16:30. The dark blue and light blue lines represent the liquid pumping rate and cumulative volume respectively. The red and orange lines are the measured pressure.

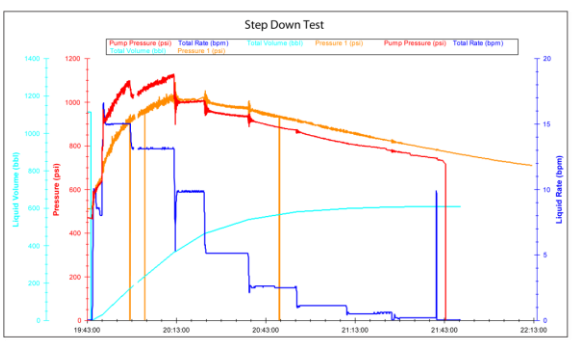

Figure 8: Step down test conditions from 19:43 to 21:30. The dark blue and light blue lines represent the liquid pumping rate and cumulative volume respectively. The red and orange lines are the measured pressure. The primary purpose of the step down test was to infer frictional losses. Frictional losses were estimated from these data and stabilized injection values were corrected for hydrostatic head and friction.

The step rate test was used to infer in-situ stress and the step down test complimented the step rate test by providing friction values for bottom hole pressure calculation and for assessing the complexity of the near-wellbore fracture regime. Figure 7 shows step rate data. Prior to this low rate injection had been carried out, starting a 0.25 bpm. After a temporary shutdown, injection was started again at approximately 5 bpm. The data in orange were measured at the wellhead and these were corrected for estimates of bottom hole pressure. After monitoring the pressure decay for after closure assessment of permeability, the step-down component of the test was performed, starting at 15 bpm.

The processed step rate data are shown in Figure 9.

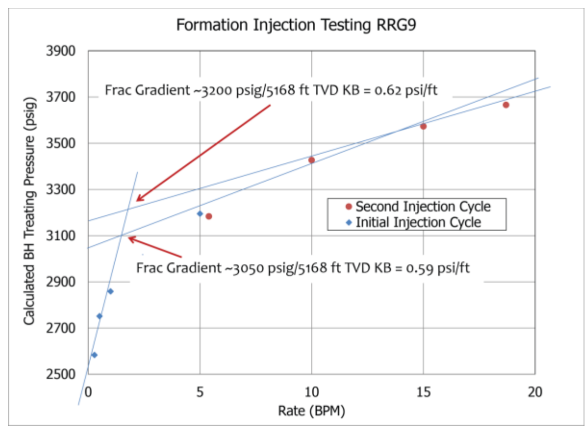

Figure 9 Stabilized bottom hole treating pressure was estimated at each injection rate and the two were crossplotted. Backwards extraction suggests substantial fracture inflow (reopening or initiation) at bottomhole pressures of approximately 3,000 psi.

Analysis of the test results, a reopening pressure of 3,050-3,200 psi. This suggested a fracture gradient between 0.59 and 0.62 psi/ft in the Elba Quartzite. In addition to the physical measurement of the in-situ stress acoustic data were processed in order to infer moduli and stresses along the logged length of the wellbore. Young's modulus was estimated from conventional dynamic relationships. It was calibrated by simple global translation to one static mechanical value that had been determined in the laboratory from core taken in RRG-3 (TerraTek 2011). Similarly, the in-situ stress inferred from the step rate measurements was used to correct the stress predictions made from measured slownesses. The raw stress data was simply inferred using concepts of the coefficient of earth pressure at rest (involving the dynamic Poisson's ratio), the estimated reservoir pressure, and the vertical total stress determined from integration of the density log. Figure 10 shows the principal stresses acting on the surrounding rock with depth.

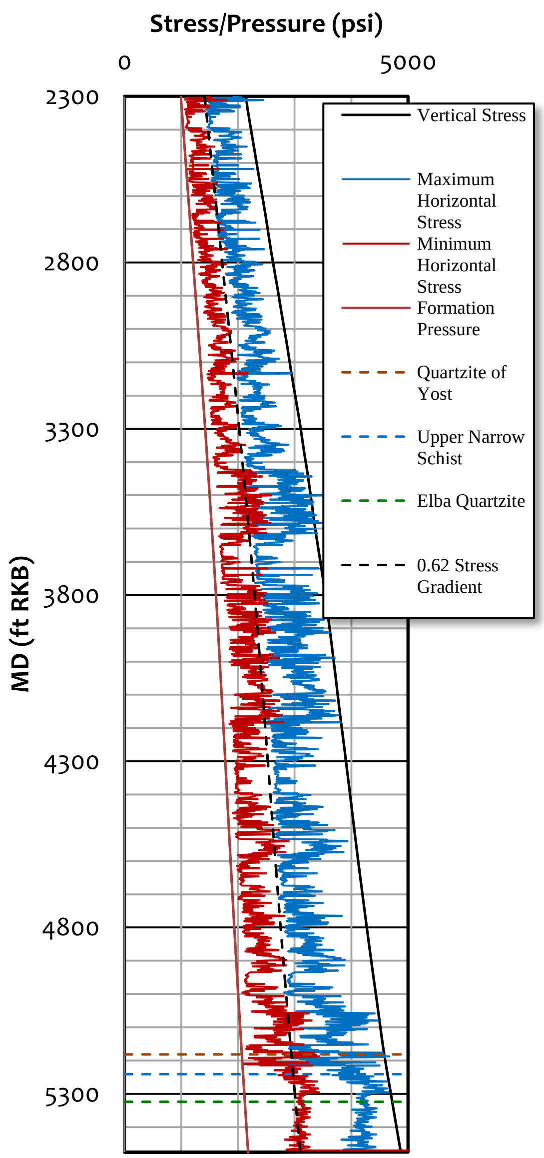

Figure 10: Stress Profile of RRG-9 ST-1. Below this depth, logging data were not available.

The stress profile was calibrated to match the results from the step rate test. It is important to note that the minimum horizontal stresses acting on the rocks above Upper Narrow Schist (top of the Precambrian basement) are generally greater than those in the Elba Quartzite. Preliminary simulations with this stress model indicate that a hydraulic fracture originating in the Elba Quartzite will remain in the formation and not grow vertically into the Upper Narrows Schist. Figure 11 is a simplified representation of how a planar hydraulic fracture would grow in this stress regime.

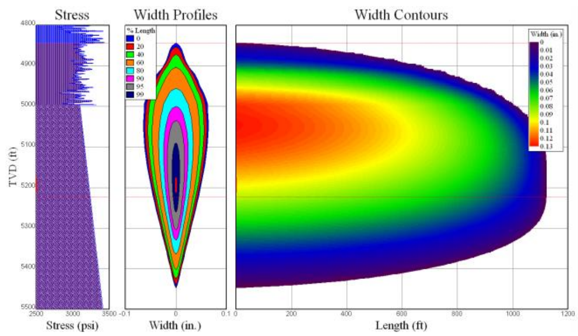

Figure 11: Simulated step rate test fracture.

The main complication was that no logging data was available in the barefoot section.

DEVELOPMENT OF A DISCRETE FRACTURE NETWORK FOR RRG-9 ST-1

While the simplified hydraulic fracturing simulation shown in Figure 11 provides some insight, it was anticipated that fabric and natural fractures will have a substantial influence on the ultimate fracture geometry – which is anticipated to be much more complicated than the planar structure shown. To enable more sophisticated assessments, some representation of the natural fracturing network was required. A televiewer log had been run prior to the step rate test. Eighty six fractures were identified in the open hole section of the well between 5,524.59 ft to 5,920.8 ft MD (Figure 12, 13 and 14).

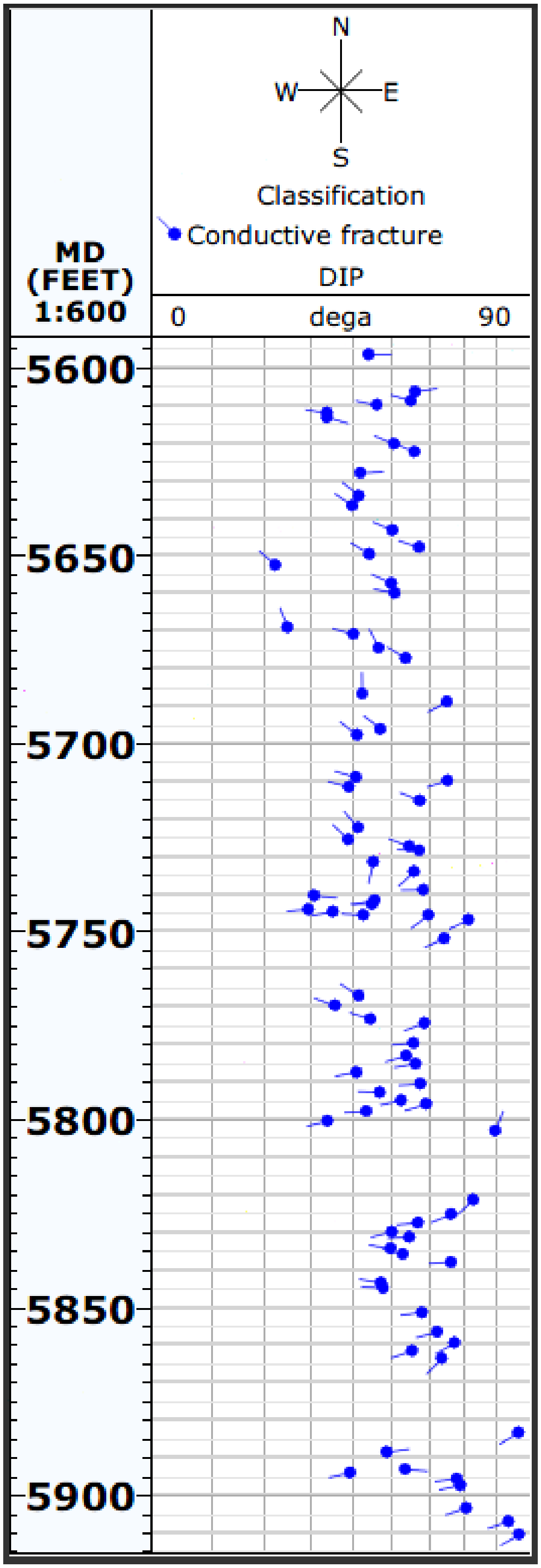

Figure 12: Tadpole diagram of identified fractures.

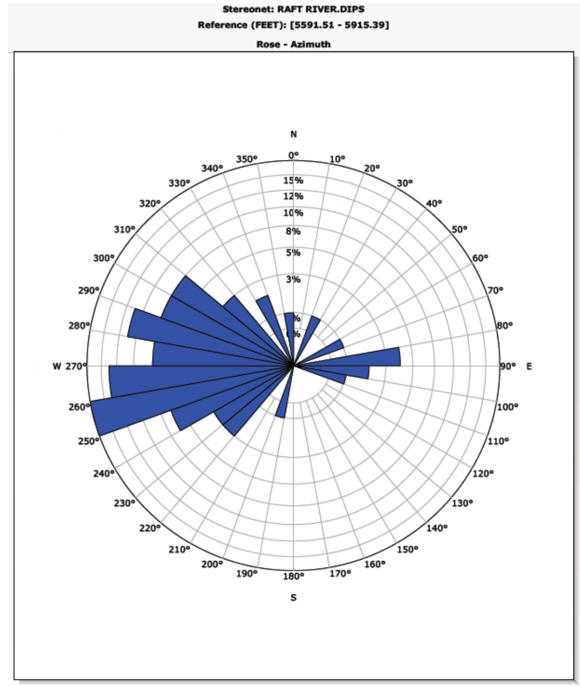

Figure 13: Fracture population dip azimuths.

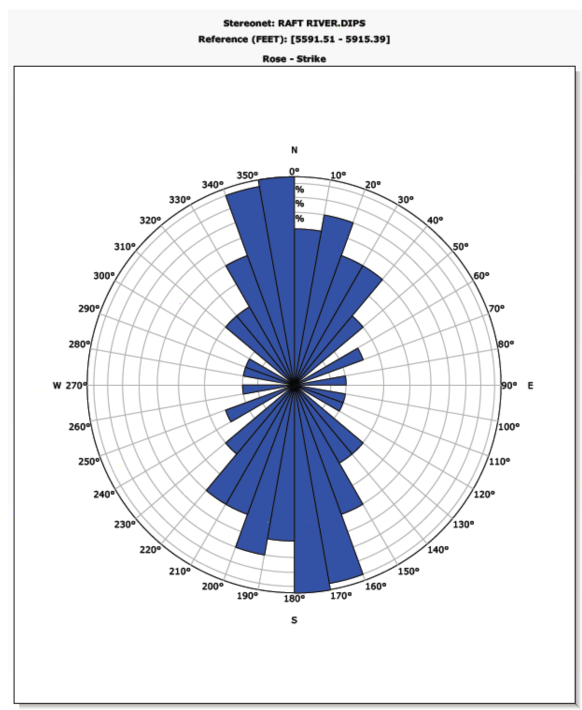

Figure 14: Fracture population dip strikes.

The fractures generally trend from N20^{0}W to N20^{0}E and dip from 40º to 60º W. Using these data and regional tectonic mapping and insights, as well as magnetic and gravity measurements a discrete fracture network was generated for the Elba Quartzite zone.

A significant finding of the televiewer survey was the dominant presence of a fractured zone imaged in the televiewer log at a depth of 5,640-60 ft within the Elba Quartzite (Figure 15).

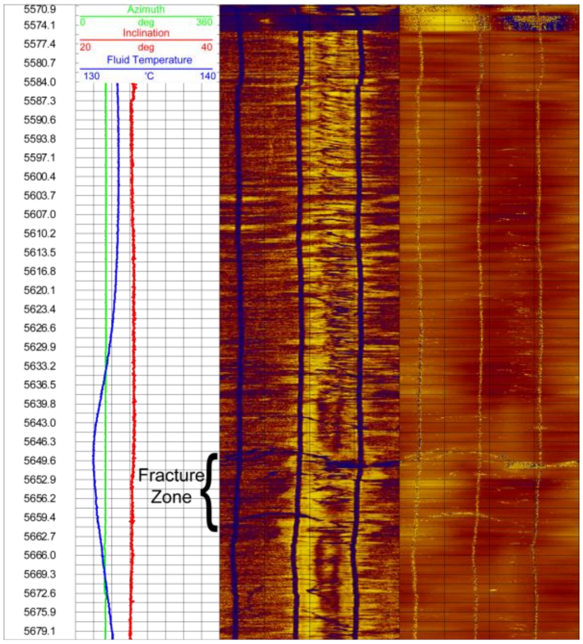

Figure 15: Televiewer image of the fracture zone at 5,645-5,660 ft. The lower temperatures within this zone result from fluid losses during drilling. These losses were not detected prior to the logging.

This zone showed slight cooling before and after injection testing, suggesting the zone was permeable. A distributed temperature perturbation survey (R. Salve, unpublished data, 2012), run approximately 2 weeks after the injection test shows that this zone had not recovered thermally at that time. Despite the apparent abundance of fractures, the zone near the top took most fluid – not surprisingly. This would be a good opportunity for using diverters.

With some subjectivity, Figure 16 displays the distributed fracture network model generated from the data.

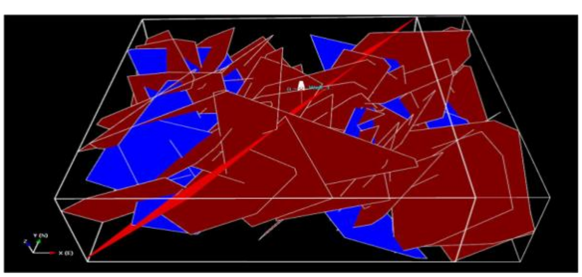

Figure 16: Image of discrete fracture network generated for RRG-9 ST-1. 72 fractures were delineated including a major feature (in red) intersecting the wellbore at between 5,640-60 ft.

The numerical simulations were conducted with the Itasca code *3DEC* (Itasca, 2011). *3DEC* is a discrete element method simulator, which represents the fractured rock mass as an assembly of deformable blocks with interfaces between them. The interfaces are representative of faults, joints and pre-existing fractures. *3DEC* simulates elastic and elasto-plastic deformation of such blocks, as well as sliding and opening of the interface between the blocks. Fluid flow in *3DEC* is simulated within a network of flow planes representing a discrete fracture network, DFN. Intact rock is assumed to be impermeable and no matrix fluid flow is calculated. Code simulations are based upon a fully coupled formulation in which the deformation of the solid phase affects the fluid pressure, and the fluid pressures affect the deformation of the matrix blocks.

The process of fluid injection was simulated in a domain of 1,000x1,000x400 ft enclosing a DFN. The model domain was comprised of three layers: one layer where the fractures were defined, and two extra layers above and below the DFN with specific mechanical properties and stress conditions. Injection was simulated by imposing a constant rate injection at the wellbore.

The central model layer was created from the provided DFN consisting of two fracture sets and a single fault plane. Figure 17 shows both a plan-view and an isometric view of the fractures (green and blue sets) and the fault plane (red).

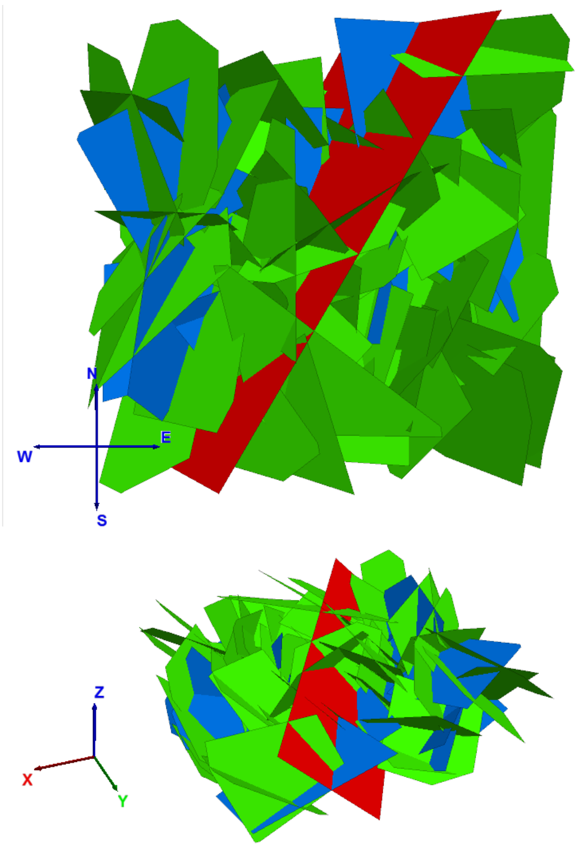

Figure 17: The figure shows three features. Blue and green, totaling 72 joints, represent the two joint sets. The polygon in red represents the fault plane. Top: Plan view of the DFN with north to the top. Bottom: Isometric view of the DFN.

A series of parametric injection simulations were conducted in order to evaluate the sensitivity of the simulation results to uncertain fracture parameters.

Figure 18 shows the injection pressure history for the simulation case presented here.

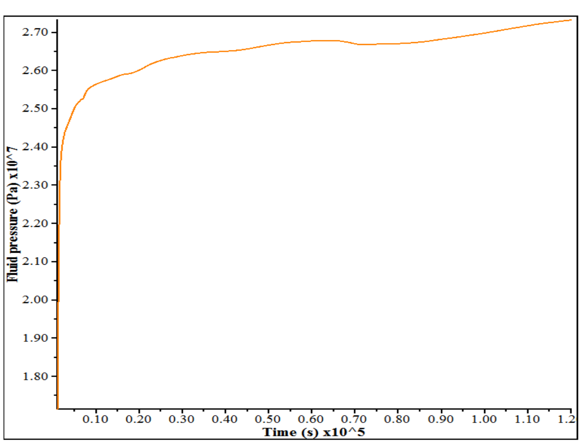

Figure 18: Wellbore injection pressure history for the simulation case presented. The injection pressure tends to level out about 6 MPa/900 psi above the in-situ minimum principal stress.

As shown in the figure, there is no sign of breakdown (common when injecting into fractured formations) and the injection pressure more or less levels out about 6 MPa (900 psi) above the in-situ minimum stress.

Figures 19 and 20 show fracture aperture and fracture pressure at the time the pressure pulse has reached the edge of the DFN domain. The majority of apertures range from 0.25 to 0.4 mm. Injection pressure is seen high at the wellbore, but rapidly drops towards the edge of the DFN domain.

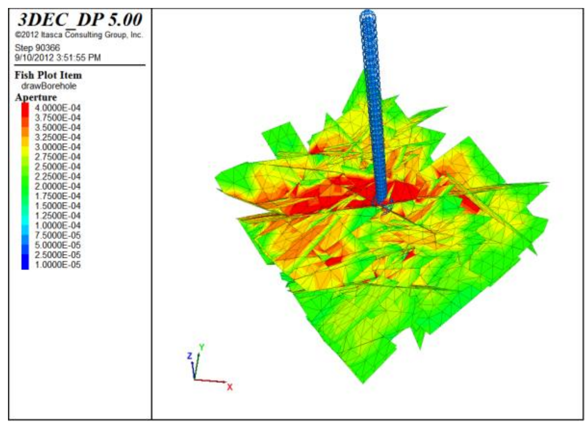

Figure 19: Fracture apertures for the simulation case presented. The majority of apertures range from 0.25 to 0.4mm.

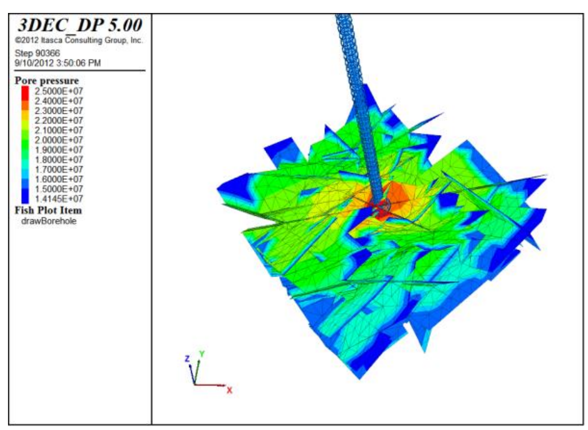

Figure 20: Wellbore injection pressures for the simulation case presented. Pressure is seen to rapidly decrease away from the wellbore.

STIMULATION PLAN

In contrast to other stimulation projects, we will conduct a series of staged stimulation treatments. During the first two stages, water at 140°F and 55°F will be injected to pre-condition and thermally fracture the reservoir. It is expected that some of the tensile thermal fractures will intersect preexisting fractures that will open and/or shear during subsequent high rate hydraulic stimulation via shear due to effective stress changes. Thus it may be possible to access a larger volume of the target region by taking advantage of the thermal stress alteration and associated fracturing. The circulation time for each of these stages is anticipated to be between 30 and 60 days. Initially the water will be injected at a rate of 5 bpm, based on the results of the step rate tests. The third stage will consist of a high rate, large volume conventional hydraulic stimulation. Microseismic, production, pressure, electromagnetic, geochemical and tracer data will be used to monitor the effects of the stimulation on the fractured volume and interconnectivity.

CONCLUSIONS

Stimulation of RRG-9 ST-1, located in the Raft River geothermal field Idaho, provides an opportunity to assess the viability of thermal stress alteration combined with hydraulic fracturing to develop enhanced geothermal system reservoirs. The well was drilled to a total depth of 5,932 ft. Eighty-six naturally occurring fractures trending from N20^{o}W to N20^{o}E and dipping from 40^{o} to 60^{o}W were identified in the open hole section of the well between 5,551 and 5,932 ft. Step rate testing suggests a fracture gradient of 0.59 to 0.62 psi/ft and minimum reopening pressures of 3,050-3,200 psi. The fracture zone between 5,540 and 5,560 ft accepted most of the fluid during the step rate test. A preliminary earth model of the site, which includes stress data and a discrete fracture network, has been developed. The stimulation of the well is scheduled for 2013. It will consist of three stages: low pressure injection of 140^{o}F water (stage 1), low pressure injection of 55^{o}F water (stage 2) and hydraulic fracturing (stage 3).

ACKNOWLEDGEMENTS

The authors are grateful to the management and staff of U.S. Geothermal Inc. for their support and assistance. This work was funded under DOE Grant DE-FG36-08GO18189.

REFERENCES

Ayling, B., Molling, P., Nye, R. and Moore, J. (2011), “Fluid geochemistry at the Raft River geothermal field, Idah: New data and hydrogeological implications,” *Proceedings: Thirty-Sixth Workshop on Geothermal Reservoir Engineering*, Stanford University, SGP-TR-191.

Covington, H. R. (1983), “Structural evolution of the Raft River Basin, Idaho,” *Geological Society of America*, 229-237.

Itasca. (2012), “Numerical Simulation of a Hydraulic Fracture Stimulation for Geothermal Operations,” *Unpublished report to Energy & Geoscience Institute at the University of Utah.*

Keys, W. S. (1980), “The Application of The Accoustic Televiewer To The Characterization Of Hydraulic Fractures In Geothermal Wells,” *Geothermal Reservoir Well Stimulation Symposium*, (pp. 176-202). San Francisco.

Maris, V., Wannamaker, P. E. and J. Moore. (2012), “3-D inversion of MT data from the Raft River Geothermal Field – Preliminary results,” *Energy & Geoscience Institute at the University of Utah GRC paper*.

Salve, R. and Freifeld, B. (2012), “Thermal Logging of RRG-9 Using a Distributed Thermal Perturbation Sensor,” *Unpublished report to the Energy & Geoscience Institute at the University of Utah.*

TerraTek. (2011), *“Rock Materials Testing RRG-3.”Unpublsihed report to the Energy & Geoscience Institute at the University of Utah*